

Regulatory role of HSP60 in scavenger receptor mediated atherogenic changes in THP-1 macrophages

Introduction

Macrophages form integral component of atheromatous plaques and are involved in all the stages of atherosclerosis development. The earliest presence of macrophages at the site of lesion formation is believed to be resulting from endothelial dysfunction induced recruitment of monocytes in the sub-endothelial space (Xu et al., 2019). These monocytes differentiate into macrophages under the influence of chemokines secreted by the dysfunctional endothelium (Clinton et al., 1992; Rajavashisth et al., 1990). In addition, endothelial damage also facilitates the intimal transcytosis and free radical mediated oxidation of LDL molecules to form oxidized LDL (OxLDL) (Vasile et al., 1983; Yoshida and Kisugi, 2010). The macrophages actively participate in ingestion and accumulation of OxLDL leading to formation of lipid-laden foam cells, the hallmark of atherosclerosis. The transformation of macrophages to foam cells affects its phenotype and function leading to inflammatory changes (Shashkin et al., 2005). Formation of foam cells is a key event in atherosclerosis because it reduces the macrophages' ability to migrate leading to failure of inflammation resolution that majorly contributes in atherogenic progression (Huang et al., 2014; Park et al., 2009). Hence, an understanding of molecular events regulating the uptake of lipids and subsequent formation of foam cells is imperative for profound understanding of the disease.

The cytosolic accumulation of OxLDL in macrophages is mediated via scavenger receptors dependent phagocytosis and pinocytosis (Chistiakov et al., 2016). Amongst others, SR-A1 and CD36 contribute to about 90% of OxLDL uptake making them the principal

contributors to macrophage cholesterol accumulation (Kunjathoor et al., 2002). It is well-established that OxLDL also enhances its uptake by macrophage via upregulation of SR-A1 and CD36 expression (Han et al., 1997; Lara-Guzmán et al., 2018). The degree of accumulation is also affected by cholesterol efflux involving scavenger receptor class B type 1 (SR-B1) (Shen et al., 2018). Deletion of SR-B1 has been reported to increase atheromatous plaque size by about 86% and overexpression of the same receptor showed a decrease in the lesion formation (Zhang et al., 2003). SR-B1 mediates the efflux of cholesterol to HDL molecules for elimination through reverse cholesterol transport (Kinoshita et al., 2004). Thus, a skewed balance between the functioning of scavenger receptors and subsequent impact on influx and efflux of lipids majorly contribute to intracellular lipid accumulation and disease progression.

The excessive accumulation of modified lipids affects the cellular fate of macrophages, since they are known to polarize into distinct subtypes based on the immunological stimulus in their immediate surroundings. In a rather simplified view, polarization of macrophages give rise to two major sub-types namely, M1 and M2 wherein, M1 macrophages exhibit inflammatory phenotype and M2 macrophages are the anti-inflammatory ones (Martinez et al., 2008). Since atherosclerotic plaques are characterized by non-resolved inflammation, it can be assumed that they may be rich in inflammatory M1 macrophages. However, studies with murine as well as human lesions have shown the presence of both M1 and M2 macrophages within the plaque. The distinct spatial distribution of these macrophage subsets emphasizes the significance of microenvironment in macrophage polarization. Interestingly, foamy macrophages in atherosclerotic plaques of mice have been found to express ambiguous repertoire of both M1 (inflammatory) and

M2 (anti-inflammatory) markers (2012-distribution of macrophage markers in plaques) (Stöger et al., 2012). Further, scavenger receptors have also been reported to act in concert with Toll-like receptors (TLRs) activating a downstream pro-inflammatory cascade generating mature IL-1 β via NLRP3 inflammasome (Moore et al., 2013; Stewart et al., 2010). Also, M2 macrophages have been shown to express high levels of scavenger receptors, making them more susceptible to OxLDL uptake and foam cell formation (Oh et al., 2012). In light of the available reports, it can be said that the mechanisms driving the macrophage polarization in atherogenic conditions is rather complex and it is imperative to scrutinize the precise biochemical and regulatory pathway resulting in ambiguous polarization of macrophages in deciding the fate of atherogenic progression.

Heat shock protein 60 (HSP60) is an essential molecular chaperone that maintains cellular function by preventing misfolding and aggregation of protein in conditions of stress (Hartl et al., 2011). However, immunomodulatory properties of HSP60 have been identified that triggers inflammatory immune reactions crucial for initiation and progression of atherosclerosis (Matsuura et al., 2009). In this context, stress induced secretion of HSP60 from vascular cells is of prime importance as soluble HSP60 is known to activate toll like receptor 4 (TLR-4) mediated inflammatory pathway in macrophages (Ohashi et al., 2000). Further, macrophage activation by HSP60 has also been linked with its ability to bind TLR-2 and CD14 (Vabulas et al., 2001) (Kol et al., 2000). Also, surface expression of HSP60 in atherosclerotic conditions have been identified as a trigger for activating innate and adaptive immune responses that contributes to atherogenic progression (Cohen-Sfady et al., 2005; Osterloh et al., 2008; Quintana and Cohen, 2011).

Apart from the immunological interactions of extracellular HSP60 with macrophages, its intracellular modulations have also been reported to have consequences that are important in atherogenesis. Recently, hyperglycemia mediated upregulation and subsequent secretion of HSP60 from THP-1 monocytes have been observed to induce paracrine inflammatory reaction in endothelial cells (Martinus and Goldsbury, 2018). Further, the limited information available on intracellular HSP60 modulations have been obtained from studies in endothelial cells and smooth muscle cells (Amberger et al., 1997; Choi et al., 2015; Zhao et al., 2015). However, the role of intracellular HSP60 modulations with atherogenic manifestations in vascular cells is poorly understood. Interestingly, we had observed HSP60 upregulation mediated regulation of endothelial dysfunction and activation affecting subsequent recruitment of monocytes (chapter 2). In light of available reports and our observations in endothelial cells, we hypothesize that intracellular HSP60 modulations possibly has a regulatory role in macrophages. Since OxLDL induced HSP60 upregulation in monocytic cell lines has been observed (Frostegard et al., 1996), herein, we hypothesize that HSP60 has a bigger role in foam cell formation.

In this study, we had investigated the modulatory role of HSP60 on accumulation of OxLDL in THP-1 monocyte derived macrophages (MDMs) via scavenger receptors and its impact on macrophage polarization.

Materials and methods

Experimental model: THP-1 monocytes were seeded at a density of 1.5×10^6 cells/ml with 50nM PMA (phorbol 12-myristate 13-acetate) in serum-free RPMI-1640 medium for 24 h. This differentiated the cells to M₀ macrophages that were termed as THP-1 monocyte derived macrophages (MDMs).

OxLDL doses:

- 8 µg/ml corresponds to the lower limit of serum levels of OxLDL that had been recorded in patients with atherosclerosis (Chen and Khismatullin, 2015).
- 80 µg/ml represents a dose that has been observed to show lipid accumulation with minimal toxicity in THP-1 macrophages (Liu et al., 2016).

Experimental protocol

(i) Study I:

Experimental groups:

1. Control: untreated MDMs
2. OxLDL: MDMs treated with 8 or 80 µg/ml OxLDL in serum-free media for 24 h
3. Heat Shock: MDMs exposed to 42°C for 20 min followed by incubation at 37°C for 6 h (positive control for heat shock proteins)

Parameters tested:

1. Cell viability
2. Quantitative RT-PCR: HSP60, HSP10, HSF-1, GAPDH
3. Immunoblotting: HSP60, β-actin
4. ELISA: HSP60

(ii) Study II:

Experimental groups:

1. KD-Control: MDMs transfected with *pSilencer 2.0-U6 Negative Control* containing scrambled shRNA sequence for 48 h

2. HSP60 KD: : MDMs transfected with pshRNA-609 plasmid for 48 h (HSP60 knockdown)
3. OxLDL (8 µg/ml): KD-Control MDMs treated with 8 µg/ml OxLDL in serum free media for 24 h
4. OxLDL (80 µg/ml): KD-Control MDMs treated with 80 µg/ml OxLDL in serum free media for 24 h
5. HSP60 KD + OxLDL (8 µg/ml): HSP60 KD MDMs treated with 8 µg/ml OxLDL in serum free media for 24 h
6. HSP60 KD + OxLDL (80 µg/ml): HSP60 KD MDMs treated with 80 µg/ml OxLDL in serum free media for 24 h

Parameters tested:

1. Cell Viability
2. Quantitative RT-PCR: HSP60, SR-A1, CD36, SR-B1, iNOS, IL-6, Arg-1, IL-10, GAPDH
3. JC-1 staining
4. Oil red O staining and quantification

The detailed experimental protocol for the present study is depicted in Fig. 3.1. Descriptive methodology for each parameter is described in materials and methods section.

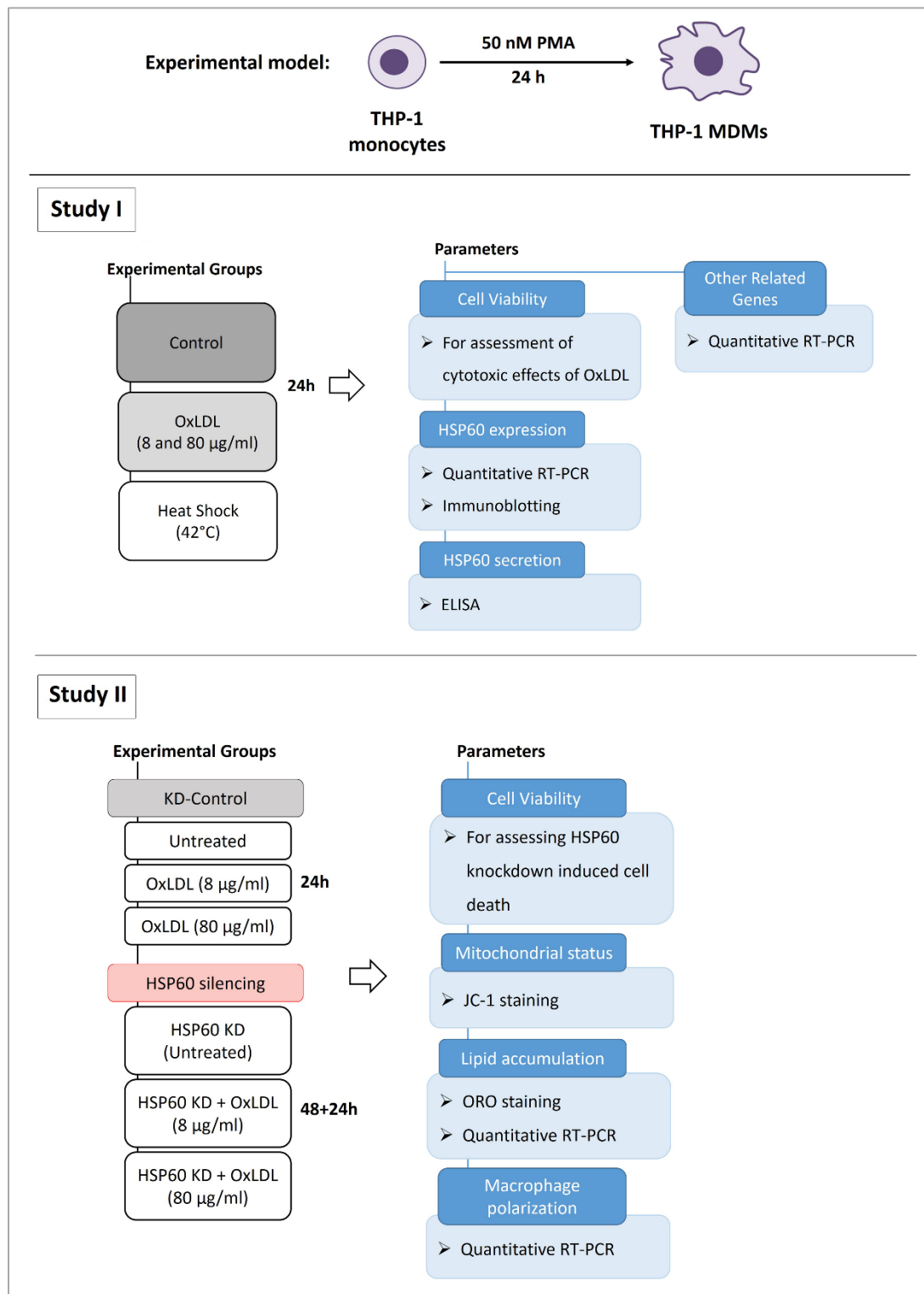


Figure 3.1: Schematic representation of experimental protocol followed for studying atherogenic events in macrophages.

Results

Cytotoxicity of OxLDL in THP-1 MDMs

THP-1 MDMs were treated with a lower dose (8 µg/ml) and a higher dose (80 µg/ml) of OxLDL for 24 h and cell viability was assessed by MTT assay. The results of MTT assay showed non-significant loss (~9%) of cell viability at lower dose of OxLDL as compared to control, whereas higher dose caused a significant decrement (~29%) in cell viability as compared to control (Fig. 3.2).

OxLDL upregulates HSP60 in THP-1 MDMs

We studied the mRNA expression and protein of HSP60 in MDMs exposed to lower and higher doses of OxLDL. Significant upregulation of HSP60 mRNA expression was observed in presence of OxLDL, but, a dose-dependent response was not recorded. Lower dose of OxLDL recorded ~12 fold upregulation in HSP60 mRNA whereas higher dose showed ~9 fold increase in the same as compared to control (Fig. 3.3a). Exposure of MDMs to heat shock (42°C; positive control), induced ~5.7 fold increase in HSP60 mRNA (Fig. 3.3b). Thus, it can be said HSP60 induction by OxLDL was higher than that of heat shock. Further, HSP60 protein expression was also found to be significantly elevated in OxLDL treated MDMs with similar expression observed at both the concentrations of OxLDL (Fig. 3.3c & d).

OxLDL induces HSP60 secretion in THP-1 MDMs

To determine the secretion of HSP60 under the influence of OxLDL, conditioned media of OxLDL treated MDMs was checked for presence of HSP60 using anti-HSP60 ELISA. On exposure to OxLDL for 24 h, MDMs secreted ~921 pg/ml and ~817 pg/ml HSP60 at lower and higher doses, respectively (Fig. 3.4). Further, LDH assay of OxLDL treated MDMs

did not show significant cell lysis as compared to untreated MDMs confirming that the HSP60 levels detected in conditioned media was indeed a result of active secretion (data not shown).

HSP60 downregulation aggravates OxLDL induced mitochondrial depolarization

Quantitative RT-PCR and western blot analysis showed successful knockdown of HSP60 (Fig 3.5a & b). However, the same caused a reduction in cell viability by ~24%, which further recorded a non-significant decrement of ~12% on treatment with both lower and higher doses of OxLDL (Fig. 3.5c). Further, JC-1 staining of the cells showed a marked decrement in red/green JC-1 ratio on treatment with OxLDL, thus implying towards mitochondrial depolarization. However, significantly higher red/green ratio was recorded in OxLDL treated KD-Control MDMs at 6 h as compared to 3 h time point (Fig. 3.6a & b). Further, the decrement in red/green ratio was aggravated in conditions of HSP60 knockdown at all the three (3 h, 6 h, and 24 h) time points (Fig. 3.7a & b).

HSP60 downregulation enhances OxLDL uptake in MDMs

The results of Oil red O staining showed a significant increase in cytoplasmic lipid droplets after 24 h of OxLDL exposure (at higher dose) as compared to untreated KD-Control. Interestingly, exposure to both the doses of OxLDL accounted for a significantly higher lipid accumulation (~23% and ~42%, respectively) in HSP60 KD MDMs compared to that in untreated KD-Control (Fig. 3.8a & b). To understand the augmented lipid accumulations observed in HSP60 KD MDMs, the mRNA expression of scavenger receptors were analyzed. As shown in Fig. 3.9a, higher dose of OxLDL significantly increased SR-A1 mRNA levels (~4.8 fold) in KD-Control MDMs. Knockdown of HSP60 induced a significant increment (~5.7 fold) in SR-A1 mRNA levels that further increased dose-

dependently (~8.3 and ~13.1 fold at lower and higher doses, respectively) on treatment with OxLDL (Fig. 3.9a). Further, a significant increment in CD36 mRNA (~2.8 fold) was noted in KD-Control MDMs on treatment with higher dose of OxLDL. But lower dose did not record a significant change. On the contrary, a dose-dependent upregulation of CD36 was observed (~4 and ~12.7 fold at lower and higher doses, respectively) in OxLDL treated HSP60 KD MDMs (Fig. 3.9b). We also observed a significant upregulation of ~2.1 and ~4.3 fold in SR-B1 mRNA expression on exposure of KD-Control MDMs to lower and higher doses of OxLDL, respectively. However, OxLDL exposure did not record significant induction in SR-B1 mRNA levels (~1.3 and ~1.8 fold at lower and higher doses, respectively) in HSP60 KD MDMs compared to untreated KD-Control (Fig. 3.9c). Interestingly, comparative analysis revealed that in conditions of HSP60 downregulation, treatment with OxLDL induced aggravated levels of SR-A1 and CD36 compared to that in KD-Control MDMs. Also, OxLDL mediated upregulation of SR-B1 was prominently reduced in HSP60 KD compared to that in KD-Control MDMs (Fig. 3.9d).

HSP60 downregulation enhances OxLDL induced inflammatory phenotype

Macrophage polarization events were studied by assessing the mRNA expression of M1 (iNOS and IL-6) and M2 (Arg-1 and IL-10) macrophage markers. The results showed that OxLDL induced a significant increment in iNOS mRNA at higher dose (~2.6 fold) with non-significant downregulation at lower dose in KD-Control MDMs. However, HSP60 KD decreased iNOS expression by 0.85 fold (non-significant) which was significantly increased on exposure to OxLDL at both doses (~2.8 and ~2.6 fold respectively) (Fig. 3.10a). In addition, mRNA levels of inflammatory cytokine (IL-6) recorded a significant upregulation (~11.4 fold) on treatment with higher dose of OxLDL compared to untreated

KD-Control. However, downregulation of HSP60 caused ~13.9 fold increase in IL-6 mRNA compared to untreated KD-Control and OxLDL treatment further increased the expression by ~31.5 and ~41.5 fold at lower and higher doses, respectively (Fig. 3.10b). On the contrary, mRNA levels of Arg-1 decreased significantly in OxLDL treated MDMs compared to untreated KD-Control MDMs. Also, HSP60 KD led to a significant decrement in Arg-1 mRNA expression as compared to KD-Control. But OxLDL treatment to HSP60 KD MDMs did not record a significant change in Arg-1 levels compared to untreated HSP60 KD MDMs (Fig. 3.10c). Similarly, the mRNA expression of anti-inflammatory cytokine, IL-10 was reduced in response to OxLDL (at both concentrations) compared to untreated KD-Control MDMs. Also, HSP60 KD significantly decreased IL-10 mRNA levels (0.06 fold) as compared to untreated KD-Control, however, OxLDL treatment in these cells restored the basal levels of IL-10 (Fig. 3.10d).

OxLDL upregulates HSP10 in THP-1 MDMs

HSP10 mRNA expression was significantly elevated in MDMs exposed to OxLDL wherein, both the doses recorded similar response (~2.8 fold). However, heat shock treatment induced a significantly higher upregulation of HSP10 mRNA expression of ~5.4 fold compared to control (Fig. 3.11).

OxLDL upregulates HSF-1 in THP-1 MDMs

OxLDL treatment (at both the concentrations) showed moderate upregulation in HSF-1 mRNA expression whereas heat shock induced a significant upregulation of ~19 fold in the same as compared to control (Fig. 3.12).

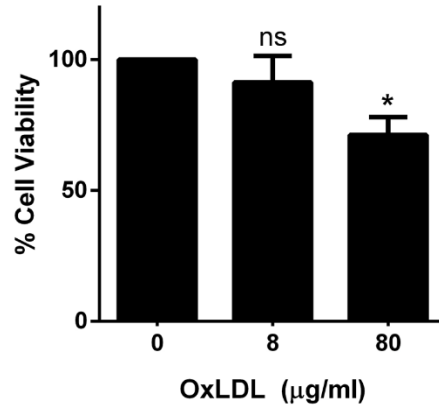


Figure 3.2: Cytotoxicity of OxLDL in THP-1 MDMs. THP-1 MDMs were treated with 8 and 80 µg/ml OxLDL for 24 h and cell viability was evaluated by MTT assay. Data were represented as Mean ± SEM (n=3). *p<0.05 vs Control, ns- non-significant.

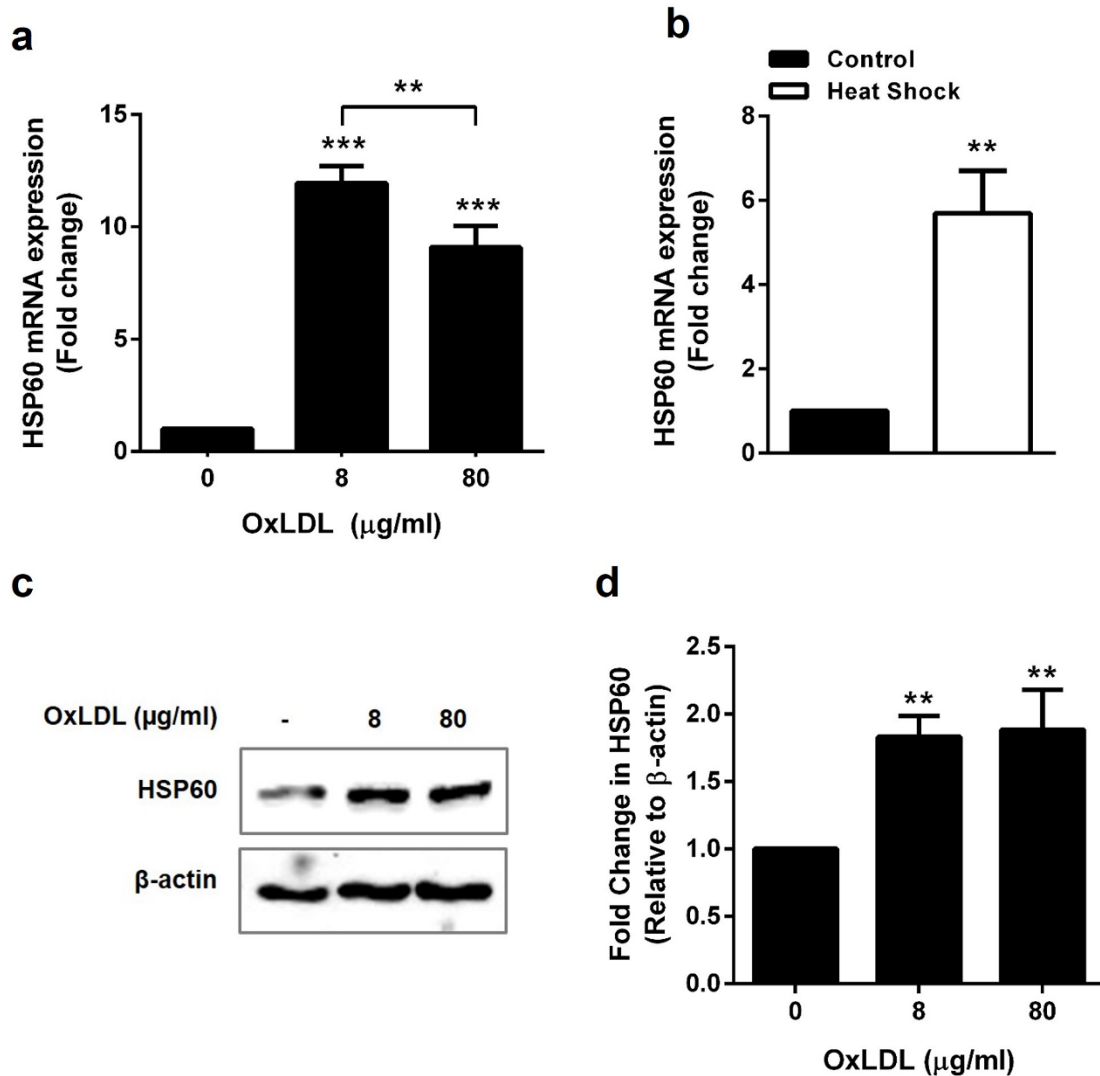


Figure 3.3: HSP60 expression in OxLDL treated THP-1 MDMs. THP-1 MDMs were treated with OxLDL (8 and 80 $\mu\text{g/ml}$) and (a) mRNA expression of HSP60 was evaluated by quantitative RT-PCR. (b) Cells exposed to heat shock (42C) were also subjected to quantitative RT-PCR for HSP60 mRNA. (c) HSP60 protein expression was assessed in OxLDL treated cells by immunoblotting and (d) bands were quantified by densitometry. Data were expressed as Mean \pm SEM (n=3). **p<0.01, ***p<0.001 vs Control.

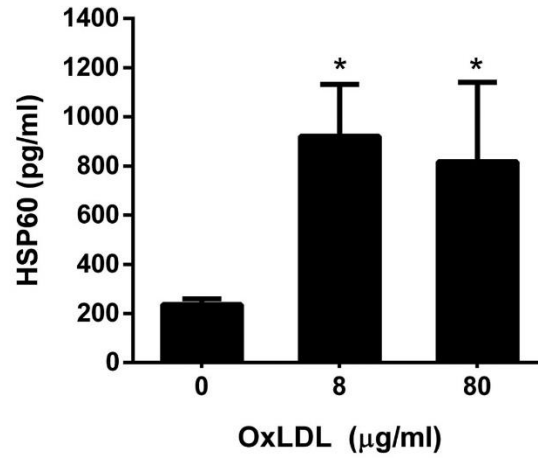


Figure 3.4: HSP60 secretion in OxLDL treated THP-1 MDMs. HSP60 levels were assessed in conditioned media of THP-1 MDMs treated with 8 and 80 µg/ml OxLDL for 24 h by ELISA. Data were represented as Mean ± SEM (n=3). *p<0.05 vs Control.

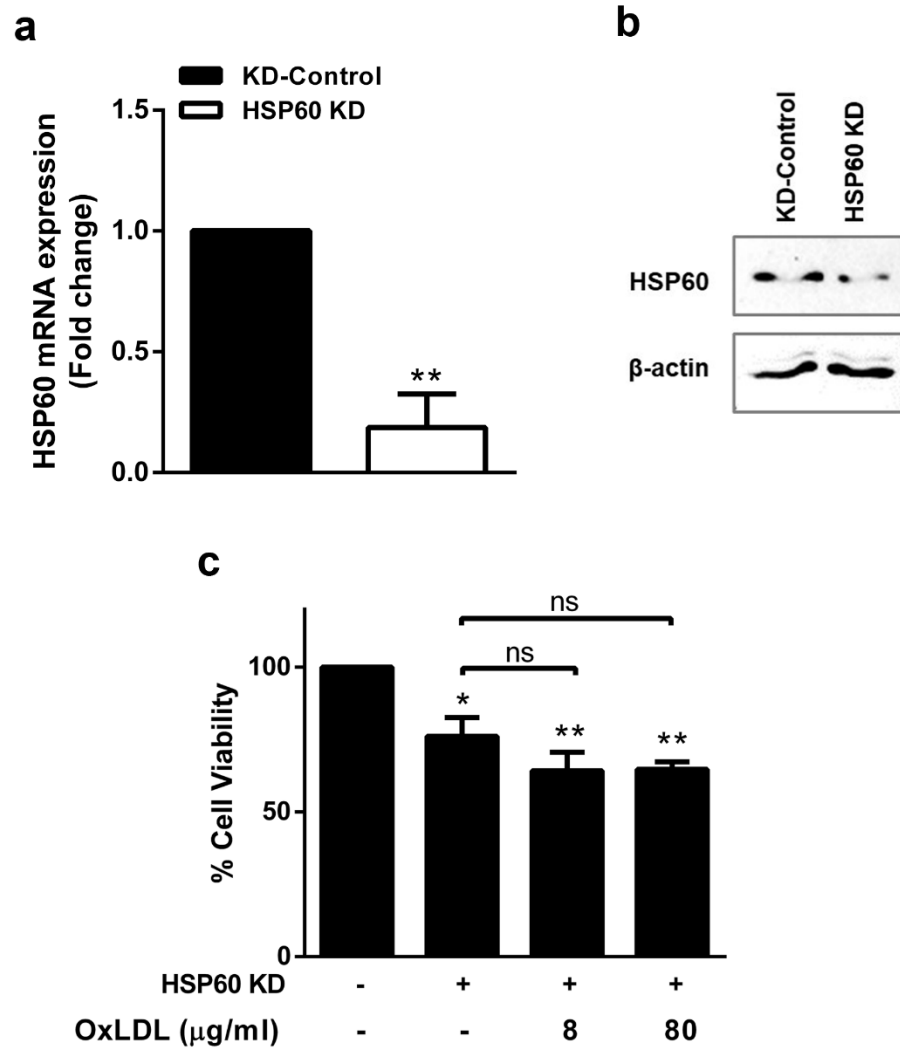


Figure 3.5: HSP60 knockdown in THP-1 MDMs. THP-1 MDMs were transfected with negative control (KD-Control) or shRNA against HSP60 (HSP60 KD) and knockdown efficiency determined by checking the (a) mRNA expression by quantitative RT-PCR and (b) protein expression by western blotting. (c) Cell viability of HSP60 KD MDMs treated with OxLDL was determined by MTT assay and % cell viability was calculated relative to KD-Control MDMs. Data were expressed as Mean \pm SEM (n=3). *p<0.05, **p<0.01 vs KD-Control.

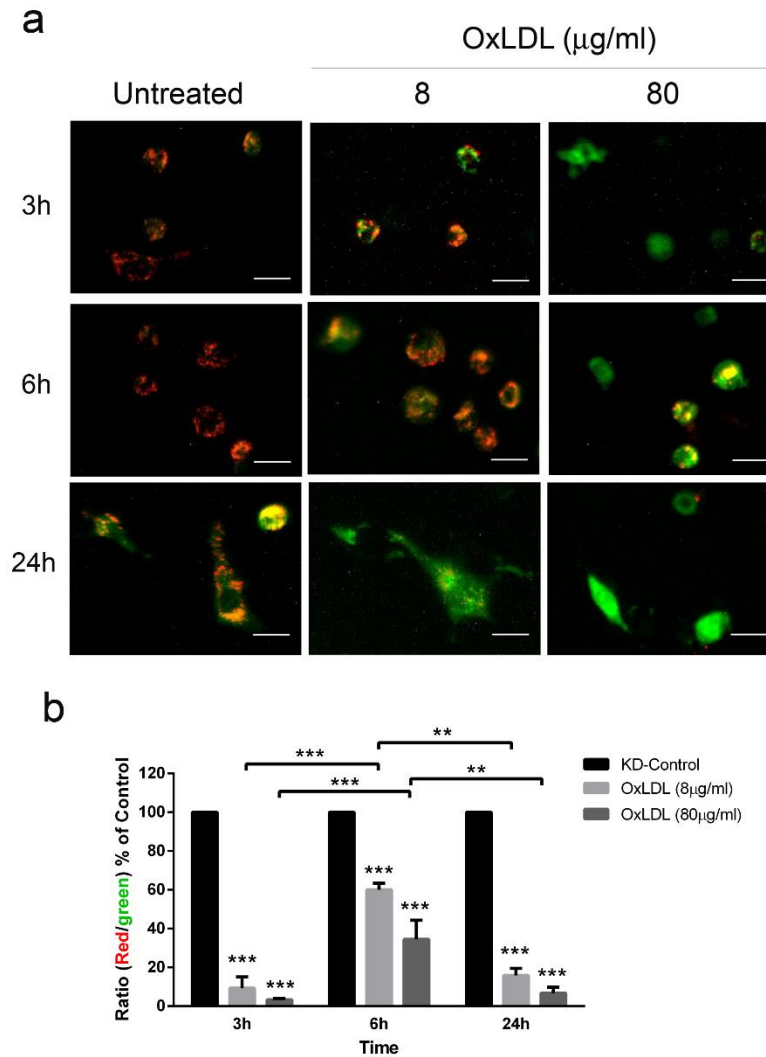


Figure 3.6: OxLDL induced mitochondrial depolarization in THP-1 MDMs. Mitochondrial membrane potential was assessed in KD-Control cells treated with OxLDL for 3 h, 6 h and 24 h using JC-1 stain. (a) Representative images of JC-1 stained MDMs are shown. Scale bar= 20 μm . (b) The red/green fluorescence ratio calculated from the images is depicted graphically. Data were expressed as Mean \pm SEM (n=3). *p<0.05, ***p<0.001 vs untreated KD-Control.

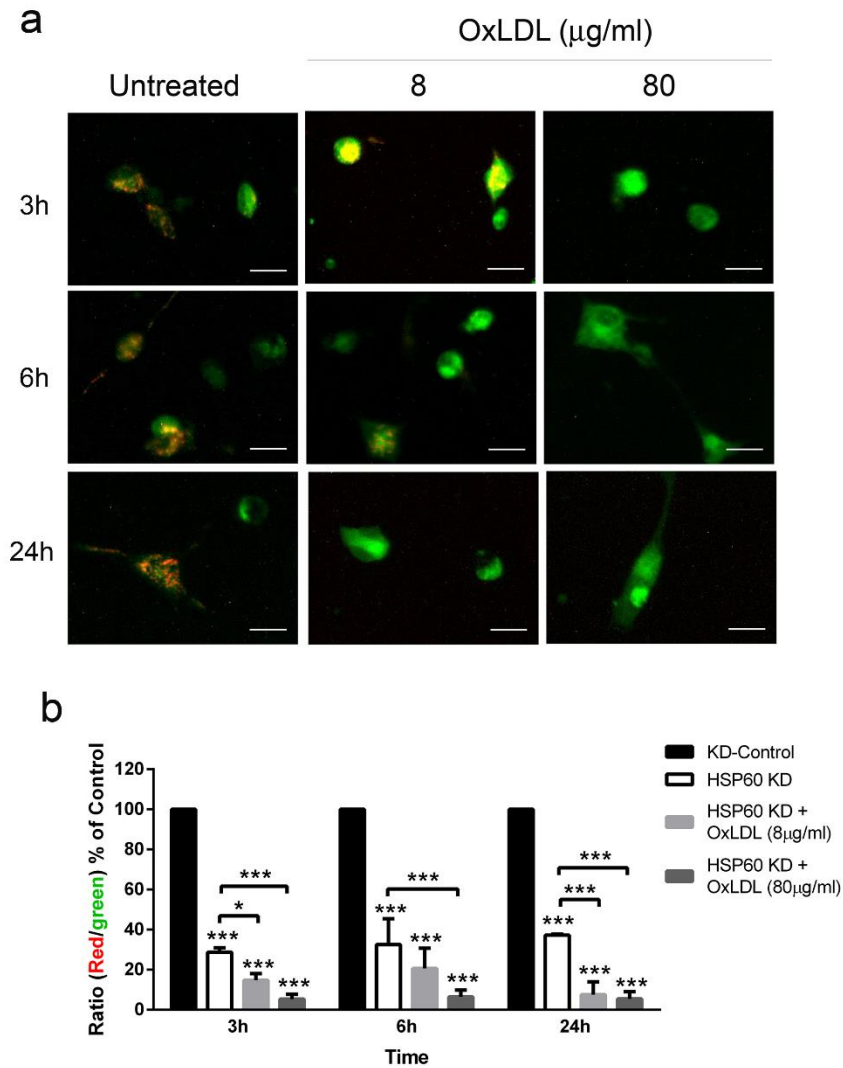


Figure 3.7: OxLDL induced mitochondrial depolarization in HSP60 knockdown MDMs. Mitochondrial membrane potential was assessed in HSP60 KD MDMs treated with OxLDL for 3 h, 6 h and 24 h using JC-1 stain. (a) Representative images of JC-1 stained MDMs are shown. Scale bar= 20 μm . (b) Red/green fluorescence ratio calculated from the images is depicted graphically. Data were expressed as Mean \pm SEM (n=3). *p<0.05, ***p<0.001 vs untreated KD-Control.

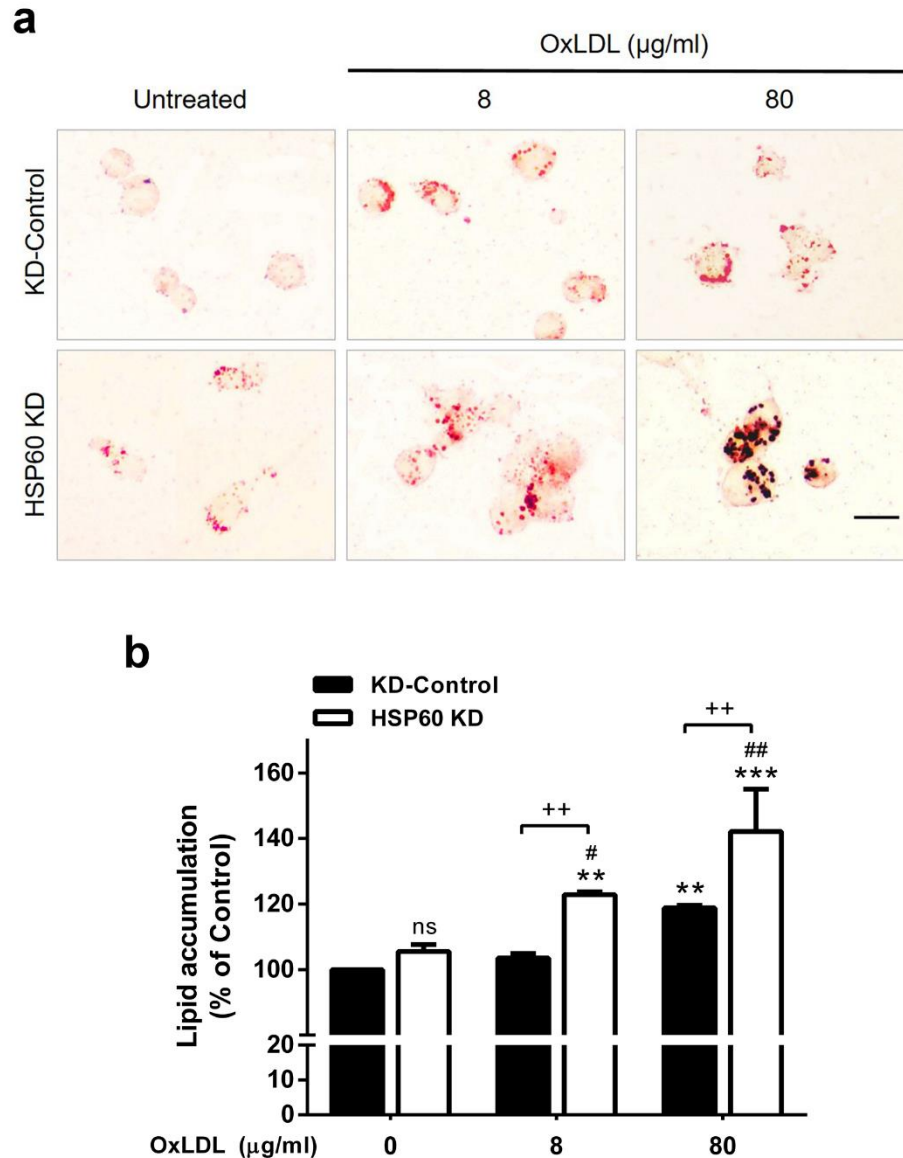


Figure 3.8: OxLDL uptake in HSP60 knockdown MDMs. Cells were subjected to Oil Red O staining to check the OxLDL uptake (a) Representative images of stained cells (Scale bar= 10 μm) and (b) quantitative measurement of OxLDL accumulation are shown. Data were expressed as Mean \pm SEM (n=3). * p <0.05, ** p <0.01, *** p <0.001 vs untreated KD-Control, ## p <0.01, ### p <0.001 vs untreated HSP60 KD, +++ p <0.01 between respective KD-Control group vs HSP60 KD, ns- non-significant.

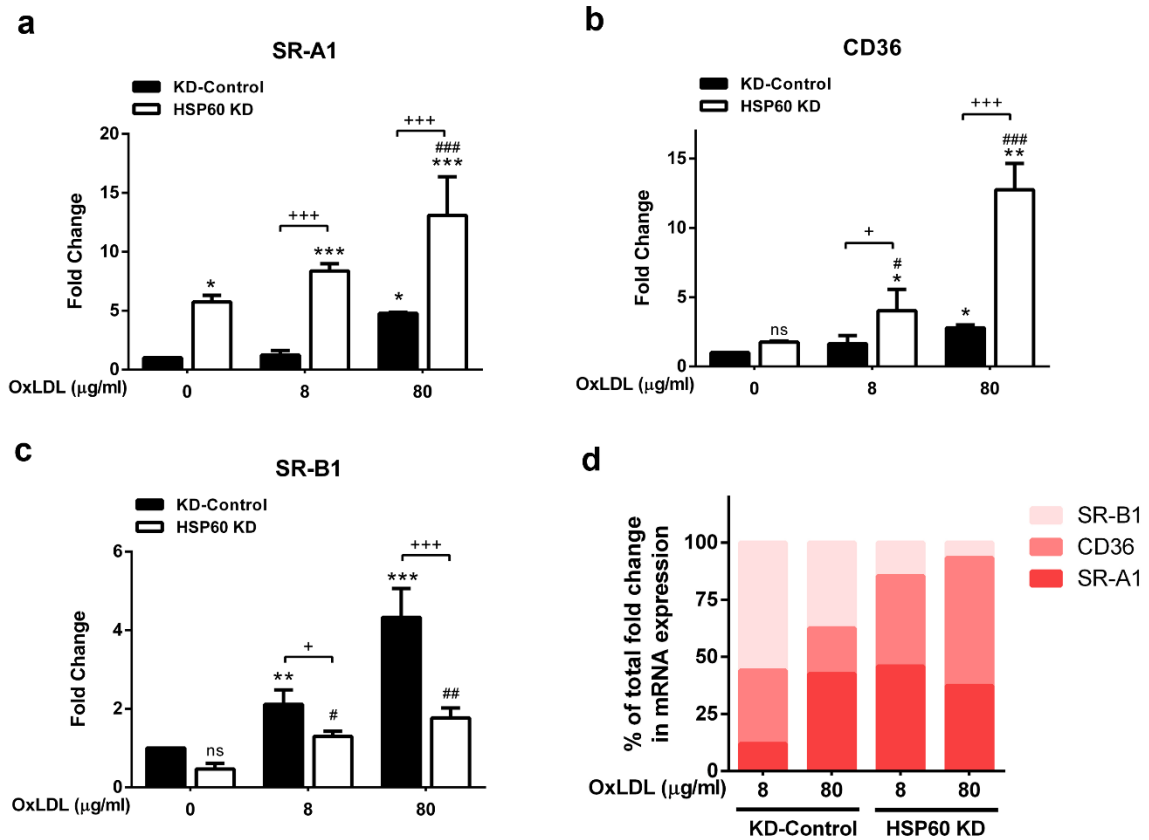


Figure 3.9: Scavenger receptors expression in HSP60 knockdown MDMs. mRNA expression of (a) SR-A1, (b) CD36 and (c) SR-B1 was evaluated in OxLDL treated KD-Control and HSP60 KD cells by quantitative RT-PCR. (d) Comparative analysis of mRNA expression of the three scavenger receptors in OxLDL treated KD-Control and HSP60 KD cells expressed as percentage of total fold change observed in respective groups. Data were expressed as Mean \pm SEM (n=3). *p<0.05, **p<0.01, ***p<0.001 vs untreated KD-Control, #p<0.05, ##p<0.01, ###p<0.001 vs untreated HSP60 KD, +p<0.05, +++p<0.001 corresponding KD-Control vs HSP60 KD groups, ns- non-significant.

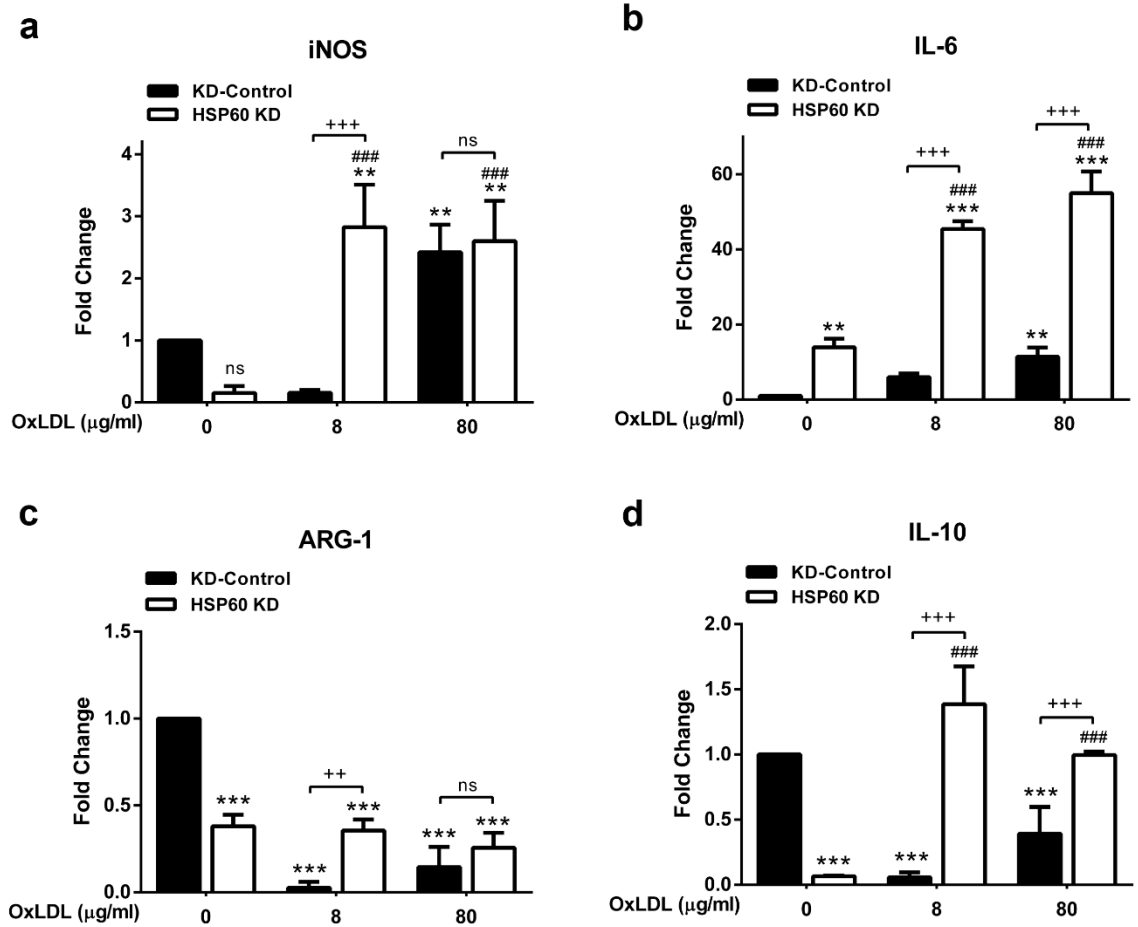


Figure 3.10: OxLDL induced polarization of HSP60 knockdown MDMs. OxLDL induced polarization events were checked by assessing the mRNA expression of M1 markers (a) iNOS and (b) IL-6 and M2 markers (c) Arg-1 and (d) IL-10 in OxLDL treated KD-Control and HSP60 KD MDMs. Data were expressed as Mean \pm SEM (n=3). **p<0.01, ***p<0.001 vs untreated KD-Control, ###p<0.001 vs untreated HSP60 KD, +++p<0.001 corresponding KD-Control vs HSP60 KD groups, ns- non-significant.

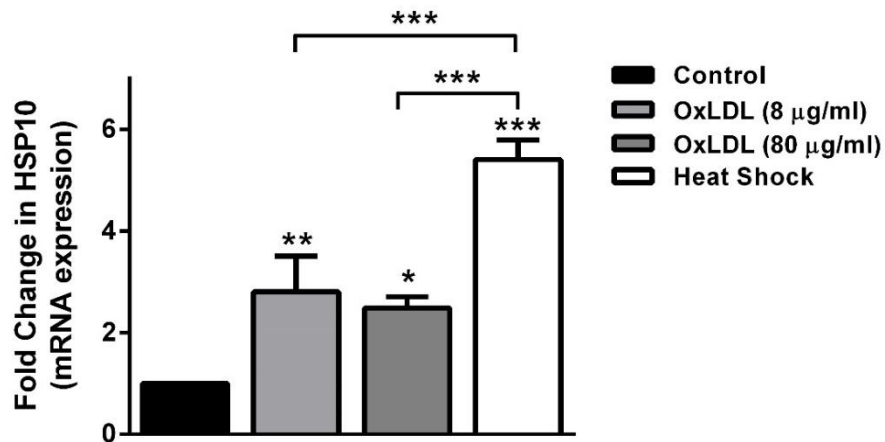


Figure 3.11: HSP10 expression in OxLDL treated THP-1 MDMs. THP-1 MDMs were treated with OxLDL (8 and 80 µg/ml) or heat shock (42°C) and the expression of HSP10 was analyzed by quantitative RT-PCR. Data were represented as Mean ± SEM (n=3). *p<0.05, **p<0.01, ***p<0.001 vs Control.

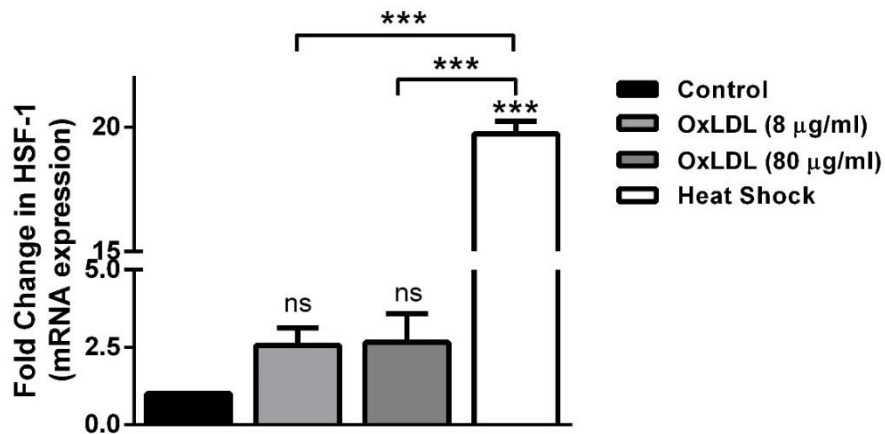


Figure 3.12: HSF-1 expression in OxLDL treated THP-1 MDMs. THP-1 MDMs were treated with OxLDL (8 and 80 µg/ml) or heat shock (42°C) and the expression of HSF-1 was analyzed by quantitative RT-PCR. Data were represented as Mean ± SEM (n=3). *p<0.05, **p<0.01, ***p<0.001 vs Control, ns- non-significant.

Discussion

Relevance of HSP60 is extensively reported in activation of immune cells including macrophages that has also been noted in human subjects and experimental models of atherosclerosis wherein, its role as a molecular regulator of atherosclerotic lesions has been emphasized (Wick et al., 2014). In this setting, hyperglycemic stress mediated release of HSP60 from THP1 monocytes has been reported (Martinus and Goldsbury, 2018) but, there is no evidence on HSP60 release from macrophages subjected to OxLDL induced stress during foam cell formation. Further, monocytes residing in the atheromatous plaque have been reported to display HSP60 overexpression (Kleindienst et al., 1993). Herein, we had observed OxLDL induced upregulation of HSP60 in THP-1 MDMs that is in agreement with reports of Frostegard et al. (1996). Similar responses recorded in lower (8 µg/ml) and higher (80 µg/ml) doses of OxLDL suggests that HSP60 upregulation and secretion is rather a sensitive event that can be triggered in macrophages even with exposure of lowest amount of OxLDL present. Further, OxLDL induced HSP60 secretion implies towards its extracellular accumulation that, along with other inflammatory cytokines, is instrumental in eliciting an immune response which stands as a preliminary event for further macrophage recruitment in the sub-endothelial space (Amberger et al., 1997; Martinus and Goldsbury, 2018; Yang et al., 2005). Paracrine action of extracellular HSP60 has also been reported (Martinus and Goldsbury, 2018) that might be relevant in augmenting atherogenic events in vascular wall.

Role of HSP60 is crucial in cell survival as a folding machinery in mitochondria wherein, its deficiency is associated with atypical mitochondrial diseases leading to multi-system failure (MacKenzie and Payne, 2007). The mitochondrial membrane potential was found

to be lowered in conditions of HSP60 knockdown that also explains the higher indices of cell death recorded in this group. Herein, it was noted that the transient improvement in mitochondrial membrane potential of OxLDL treated KD-Control MDMs at 6 h is a probable counteracting response for cell survival that was found to be lacking in conditions of HSP60 depletion.

Intracellular accumulation of OxLDL in macrophages constitutes an integral component of atherosclerosis as foam cells. Surprisingly, aggravated accumulation of lipids was observed in MDMs with HSP60 knockdown at both lower and higher doses of OxLDL, implying towards HSP60 mediated regulation of the underlying events. Interaction of modified lipids with scavenger receptors (SRs) have been known to modulate the SR expressions (Han et al., 1997; Lara-Guzmán et al., 2018). Also, coordinated activity of various scavenger receptors determine the overall lipid load in the cells. CD36 and SR-B1 are members of the same SR family that despite of being structurally related, have distinctly different functions with respect to lipid metabolism. CD36 is involved in uptake of modified lipids contributing to about 60-70% uptake in macrophages in atherogenic conditions, whereas SR-B1 actively facilitates the efflux of cholesterol from cells to HDL for elimination in bile and feces (Moore and Freeman, 2006). A comparative analysis of the SR expression in MDMs, revealed that KD-Control cells treated with lower dose of OxLDL have major contribution of SR-B1 thus, accounting for negligible intracellular accumulation of the lipids. At higher dose of OxLDL, the observed lipid accumulation was attributable maximally to the higher expression of SR-A1. Of note, comparable levels of lipid accumulation and SR-A1 expression were observed in HSP60 KD MDMs at lower dose of OxLDL. However, at higher dose, both higher CD36 and SR-A1 with lower SR-B1

expression correlated with the amount of lipid accumulation recorded in HSP60 KD MDMs. Thus, it can be said that SR-A1 and CD36 appears to be positively regulated by a lowered HSP60 status, resulting in higher indices of intracellular OxLDL accumulation. These results highlight the regulatory role of HSP60 in recruiting SRs in light of macrophage dynamics during atherogenic progression.

Accumulating evidences have revealed the presence of heterogeneous macrophage population in atherosclerotic lesions, which in turn plays key roles not only in atherosclerotic plaque progression but also in its regression (Stöger et al., 2012). Further, SRs mediated uptake of modified lipids causes an array of downstream signaling that determines the fate of macrophage phenotype (Rios et al., 2013; Van Tits et al., 2011). Since we observed HSP60 dependent regulation of SRs and the subsequent intracellular lipid accumulation, we further determined its effect on the macrophage polarization. M1 macrophages secrete inflammatory cytokines such as IL-6 and release vasoactive molecules such as nitric oxide, endothelins and eicosenoids (Aliev et al., 2001). Also, arginase-1 (Arg-1) competitively inhibits iNOS, thus cutting into the pro-inflammatory component of M1 macrophages (Mills et al., 2000) and shifting the phenotype to M2. In this study, HSP60 KD MDMs recorded significant upregulation in mRNA levels of M1 macrophage markers (iNOS and IL-6) following OxLDL treatment. These changes in inflammatory genes coincided with a significant downregulation in Arg-1 mRNA expression observed in HSP60 KD MDMs. However, these cells also recorded a significant increment in IL-10 (M2 macrophage marker) mRNA levels but, its relevance in atherogenic progression is ambiguous. Also, dual actions of M2 macrophages have been reported in atherosclerosis (Moore et al., 2013; Pello et al., 2011; Stoger et al., 2012). In

brief, our results of M1 and M2 macrophage markers imply towards a regulatory role of HSP60 wherein, HSP60 deficient macrophages account for polarization towards M1 type. However, the same needs to be scrutinized in detail in order to decipher the underlying mechanism.

Besides being an important co-factor for HSP60, it was imperative to study the modulations in HSP10 expression during foam cell formation. In the previous chapters, we had observed HSP10 upregulation in atherogenic thoracic aorta and endothelial cells. Herein, we documented the same observation in macrophages under OxLDL induced stress. However, the observed upregulation was lower compared to heat shock, a known inducer of HSPs, thereby the amounts of HSP10 in OxLDL treated MDMs appear to be merely a stress response. The moderate increment in HSF-1 in OxLDL treated MDMs is also in agreement with the stress induced response of the cells.

Overall, this study provides prima facie evidence on (a) HSP60 upregulation and release from atherogenic macrophages, (b) significantly higher indices of intracellular OxLDL accumulation in HSP60 deficient macrophages, (c) dependency on CD36 and SR-A1 for scavenging OxLDL under conditions of HSP60 deficiency and (d) polarization of macrophages towards M1 (pro-inflammatory) type that is in agreement with the said markers. Events of subtle modulations in HSP10 and HSF-1 expression warrant more experimental investigation so as to obtain conclusive evidence and find their association with HSP60 induced atherogenic processes in foam cells.